Near infrared emission from molecule-like silver clusters confined in zeolite A assisted by thermal activation

Hui, Lin
Imakita, Kenji
Sa Chu Rong Gui
Fujii, Minoru

(Citation)
Journal of Applied Physics,116:013509-013509

(Issue Date)
2014

(Resource Type)
journal article

(Version)
Version of Record

(URL)
https://hdl.handle.net/20.500.14094/90002565

Near infrared emission from molecule-like silver clusters confined in zeolite A assisted by thermal activation

Hui Lin, Kenji Imakita, Sa Chu Rong Gui, and Minoru Fujii

Citation: Journal of Applied Physics **116**, 013509 (2014); doi: 10.1063/1.4886697
View online: http://dx.doi.org/10.1063/1.4886697
View Table of Contents: http://scitation.aip.org/content/aip/journal/jap/116/1?ver=pdfcov
Published by the AIP Publishing

Near infrared emission from molecule-like silver clusters confined in zeolite A assisted by thermal activation

Hui Lin,[a] Kenji Imakita, Sa Chu Rong Gui, and Minoru Fujii[b]
Department of Electrical and Electronic Engineering, Graduate School of Engineering, Kobe University, Rokkodai, Nada, Kobe 657-8501, Japan

(Received 22 May 2014; accepted 23 June 2014; published online 3 July 2014)

Strong and broad near infrared (NIR) emission peaked at ~855 nm upon optimal excitation at 342 nm has been observed from molecule-like silver clusters (MLSCs) confined in zeolite A assisted by thermal activation. To the best of our knowledge, this is the first observation of NIR emission peaked at longer than 800 nm from MLSCs confined in solid matrices. The decay time of the NIR emission is over 10 μs, which indicates that it is a spin-forbidden transition. The ~855 nm NIR emission shows strong dependence on the silver loading concentration and the thermal activation temperature. © *2014 AIP Publishing LLC*. [http://dx.doi.org/10.1063/1.4886697]

INTRODUCTION

Molecule-like silver cluster (MLSC), or called "oligo-atomic silver cluster," which consists of several Ag atom/ions, is a kind of highly efficient luminophores in the UV-visible range and may have applications in bio-labeling,[1] white LED phosphors,[2] optical recording[3] and encoding,[4] catalysts for photodecomposition,[5,6] and dosimetry,[7,8] etc. These MLSCs can be stabilized in cryogenic inert gas,[9,10] DNAs,[11] polymers,[12] proteins,[13] glasses,[14–16] zeolites,[17–22] etc. Among them, glass and zeolite are a few kinds of solid matrices which can stabilize MLSCs. For glass matrices, it was proposed that the fluoride component, which can provide high mobility for the silver atoms and can further homogeneously precipitate MLSCs by the condensed F^- vacancies (color centers), plays an important role.[14] There also have been some reports about the characteristic ~560 nm emission from the luminescent silver species in the phosphate glass matrices.[7,8] In zeolite matrices, the mechanism of confining MLSCs is attributed to the spatially well confined cages and channels. Most of the previous work about the luminescence from MLSCs has been focused on the visible range. Though near infrared (NIR) emission has been observed from gold clusters,[23,24] reports on the NIR luminescence from MLSCs are quite few.[25,26] Here, we report strong and broad NIR luminescence peaked at ~855 nm from MLSCs confined in zeolite A matrix. The emission properties were investigated and the origin of the NIR emission was discussed.

EXPERIMENTAL

Sample preparation

Three batches of 3 g zeolite 4A (Tosoh, Japan) were weighed and stirred in a 40 ml solution of 50 mM, 150 mM, and 250 mM $AgNO_3$, respectively. The three batches of ion-exchanged zeolite powders were dried at 50 °C and then thermally treated at 150 °C, 250 °C, 350 °C, 450 °C, 550 °C, and 650 °C in air. After the thermal treatment, the powders were naturally cooled down and sealed in vials. According to the concentration of the silver nitrate solution and the thermal activation temperature, the obtained samples were named $S_{50\,mM\text{-}\times\times\times\,°C}$, $S_{150\,mM\text{-}\times\times\times\,°C}$, and $S_{250\,mM\text{-}\times\times\times\,°C}$.

Characterization

The structure of the samples was investigated by X-ray diffraction (XRD) (Rigaku, Ultima IV, Japan). Morphology of the samples was observed by field emission scanning electron microscopy (FE-SEM) (Leo 1550, Cambridge, Cambridgeshire, UK). Photoluminescence (PL) and photoluminescence excitation (PLE) spectra were measured by a spectrofluorometer (Horiba Fluorog 3 Jovin, Japan). The PL decay time under the 355 nm excitation from a third harmonic of a Nd:YAG pulse laser (5ns, 20 Hz) was measured by a photomultiplier tube (Hamamatsu, R5509–72, Japan), and the signal was analyzed with a photon-counting multichannel scaler. For all the optical measurements, the samples were loosely packed into the aluminum sample holder without any solvent.

RESULTS AND DISCUSSION

XRD θ-2θ scans of as-received pure zeolite A (S_{asp}), $S_{250\,mM\text{-}550\,°C}$, and $S_{250\,mM\text{-}650\,°C}$ are shown in Fig. 1(a). We can see that loading Ag^+ ions into the zeolite A framework and thermal activating at 650 °C do not significantly change the structure of the zeolite A framework. The characteristic cubic profile of zeolite A can be recognized and there are no obvious differences among the FE-SEM images for S_{asp}, $S_{250\,mM\text{-}550\,°C}$, and $S_{250\,mM\text{-}650\,°C}$, as shown in Figs. 1(b)–1(d). Silver nano-particles are not observed, which is in accordance with the XRD results, that is, no diffractions from silver nano-particles are observed, neither. The XRD θ-2θ scans and the FE-SEM morphology both indicate that the strong emission is from MLSCs confined in the cages of zeolite A.

To get an overall view of the emission characteristics of the MLSCs confined in zeolite A, 3D excitation-emission

[a]E-mail: linh8112@163.com
[b]E-mail: fujii@eedept.kobe-u.ac.jp

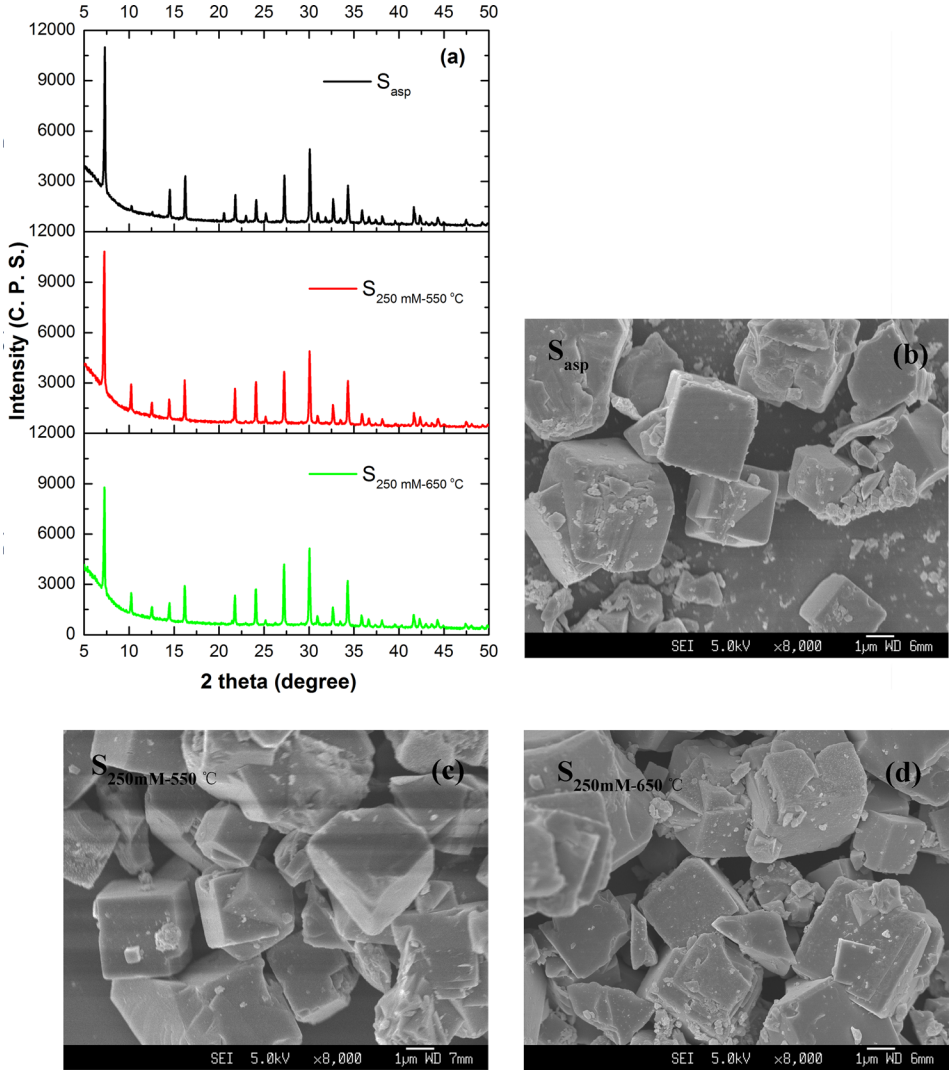

FIG. 1. XRD θ-2θ scans and FE-SEM morphology of the as-received pure zeolite A, $S_{250\,mM\text{-}550\,°C}$, and $S_{250\,mM\text{-}650\,°C}$.

contours for $S_{50\ mM\text{-}550\,°C}$, $S_{150\ mM\text{-}550\,°C}$, and $S_{250\ mM\text{-}550\,°C}$ were measured and presented in Fig. 2. In the visible range, one feature in common for $S_{50\ mM\text{-}550\,°C}$, $S_{150\ mM\text{-}550\,°C}$, and $S_{250\,mM\text{-}550\,°C}$ is that the ~560 nm emission (the yellow-green component) has an excitation band peaked at ~315 nm. Besides, for $S_{50\ mM\text{-}550\,°C}$ and $S_{150\ mM\text{-}550\,°C}$, there is another excitation band peaked at ~360 nm for the ~560 nm emission. For $S_{150\ mM\text{-}550\,°C}$ and $S_{250\ mM\text{-}550\,°C}$, a red emission peaked at ~690 nm (the red component) with the strongest excitation at ~425 nm emerged. The ~690 nm emission is not observed for $S_{50\ mM\text{-}550\,°C}$. Note that under the 315 nm excitation, there is also a blue emission peaked at 460 nm (the blue component), as shown in Fig. 4(b). The large Stokes shift and the wide emission bandwidth can be explained by the bond length change when the MLSCs are in the excited states.[14] Meantime, the contribution of electron-phonon coupling to the emission spectra broadening can also count.

For silver activated zeolite A, previously the strong ~560 nm emission was assigned to the spin-allowed singlet-singlet transition of the monovalent silver trimers (Ag_3^+) and the ~690 nm emission to a spin-forbidden doublet-quadruplet transition of the monovalent silver hexamers (Ag_6^+) located in the sodalite cage under heavy silver loading.[20] The 460 nm and 560 nm emissions were also observed in the X-ray irradiated Ag^+ activated phosphate glass and were assigned to Ag^0 atoms and Ag^{++} ions, respectively.[8] The formation of Ag^{++} ions was explained in the way of the capture of a hole by Ag^+ ion from the hole-PO_4^- pair generated upon X-ray irradiation. Unlike the MLSCs stabilized in inert gas matrices, where the number of silver atoms or ions can be exactly controlled by mass selection during the deposition process,[9] or those stabilized in organic matrices for which the number of atoms (ions) can be analyzed by mass assisted laser desorption/ionization (MALDI),[27] accurate determination of the configuration (including shape and atom (ion) number) of the MLSCs embedded in zeolites or glass matrices is more complicated. For the pioneering work, electron spin resonance (ESR) was performed to investigate the configuration of the MLSCs.[20] However, it was proved that ESR was not always powerful, for that only a few species are paramagnetic. Moreover, even for some paramagnetic MLSC species postulated from the absorption and the PL spectra like Ag_2^+ or Ag_3^{2+}, ESR signals were not observed in some situations.[19] Fortunately, it is shown that far-IR spectra[28,29] and powder XRD[30] exhibit to be good alternatives to determine the configuration of MLSCs in zeolite. Based on the conclusions in Ref. 8 (Ag^{++}), Ref. 20 (Ag_3^+), and Ref. 28

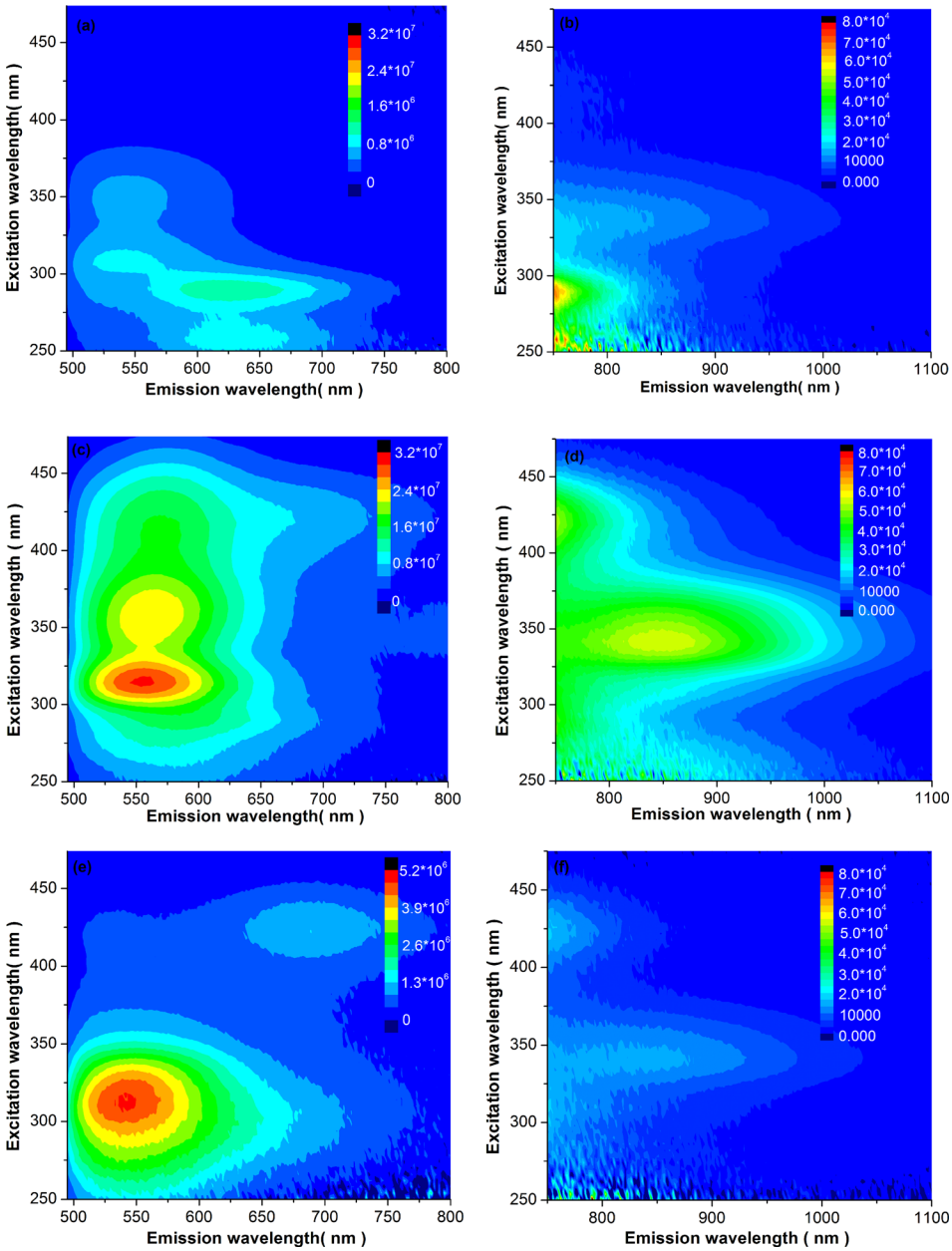

FIG. 2. 3D excitation-emission contours of the $S_{50\,mM\text{-}550\,°C}$, $S_{150\,mM\text{-}550\,°C}$, and $S_{250\,mM\text{-}550\,°C}$, excitation wavelength interval is 4 nm. Fig. 2(a), (c) and (e) were detected by the photomultiplier; Fig. 2(b), (d) and (f) were detected by the GaInAs detector.

(Ag_3^{2+}), here we tentatively assign the 460 nm and the ~560 nm emissions to Ag_3^{2+} trimers. Efforts on determining the exact species of the SCs by employing some useful tools, such as high resolution XRD and quantum chemistry modulation,[31,32] are going to be made in our future work.

In the NIR range, in Figs. 2(d) and 2(f), a broad NIR emission band peaked at ~855 nm with the optimal excitation at 342 nm is observed for $S_{150\ mM\text{-}550\,°C}$ and $S_{250\ mM\text{-}550\,°C}$. The PL band is also observed in $S_{50\ mM\text{-}550\,°C}$ (Fig. 2(b)), although the intensity is too low to see clearly in the contour image. In fact, the shape of the excitation spectra detected at 855 nm for the three samples (Fig. 3) is identical. In Ref. 14, NIR emission peaked at ~700 nm with a tail extended to 1100 nm from MLSCs confined in oxyfluoride glass has been observed. Note that the origin of this ~700 nm emission may be as the same as that of the red emission component in the silver activated zeolite A, that is, the Ag_6^{+} hexamers. However, NIR emission peaked at longer than 700 nm was not reported.[14] We believe that the strong and broad ~855 nm NIR emission from MLSCs confined in zeolite A may have various promising applications, such as the down-conversion layer to improve the conversion efficiency of crystalline silicon solar cells.

Thermal activation temperature (T_a) dependent PLE and PL spectra for the $S_{150\ mM\text{-}\times\times\times\,°C}$ series in the visible and NIR ranges are shown in Figs. 4(a)–4(d). We can see that the ~460 nm emission is dominant when T_a is $\leq$150 °C. When T_a is $\geq$250 °C, the ~560 nm emission becomes dominant instead. At the meantime, the ~855 nm emission band emerged with $T_a \geq 250$ °C and reaches maximal intensity at $T_a = 550$ °C. The strong ~560 nm emission also reaches the maximal intensity when the sample was thermally activated at 550 °C. The strongest emission intensity achieved at $T_a = 550$ °C can be attributed to the dehydration during the thermal activation which partially eliminated the highly vibrational water molecules and -OH bonds from the zeolite

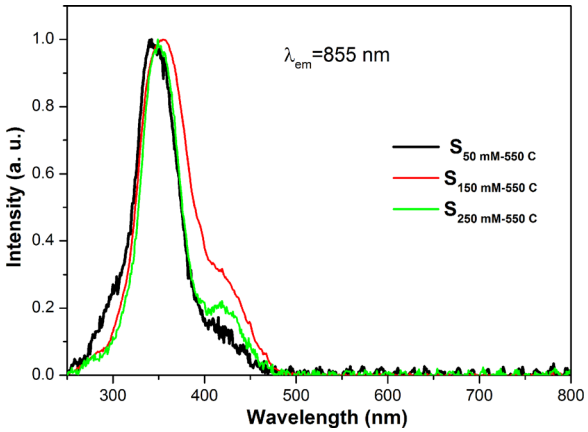

FIG. 3. Normalized PLE spectra for $S_{50\ mM\text{-}550\,^{\circ}C}$, $S_{150\ mM\text{-}550\,^{\circ}C}$, and $S_{250\,mM\text{-}550\,^{\circ}C}$, $\lambda_{em} = 855$ nm.

framework. And the emission intensity drop of $S_{150\ mM\text{-}650\,^{\circ}C}$ both in the visible and the NIR ranges implies the agglomeration of MLSCs into larger size silver species at high thermal activation temperature.

Figures 5(a) and 5(b) compare visible and NIR PL spectral shape, respectively, excited at different wavelengths. The visible emission peak wavelength shifted from 540 nm to 568 nm with the excitation wavelength (λ_{exc}) increasing from 310 nm to 460 nm. This red shift ($\Delta\lambda_{em} = 28$ nm) is much smaller compared with that of the MLSCs embedded in oxyfluoride glass ($\Delta\lambda_{em} \approx 100$ nm with λ_{exc} increasing from 320 nm to 457 nm) where the large red shift was attributed to the wide size distribution of silver clusters.[14,16] The wide size distribution for the MLSCs in oxyfluoride glass matrix has been demonstrated by energy filtered transmission electron microscopy (EFTEM) images.[14] Here, we propose another possibility for the large red shift in Ref. 14, that is, it

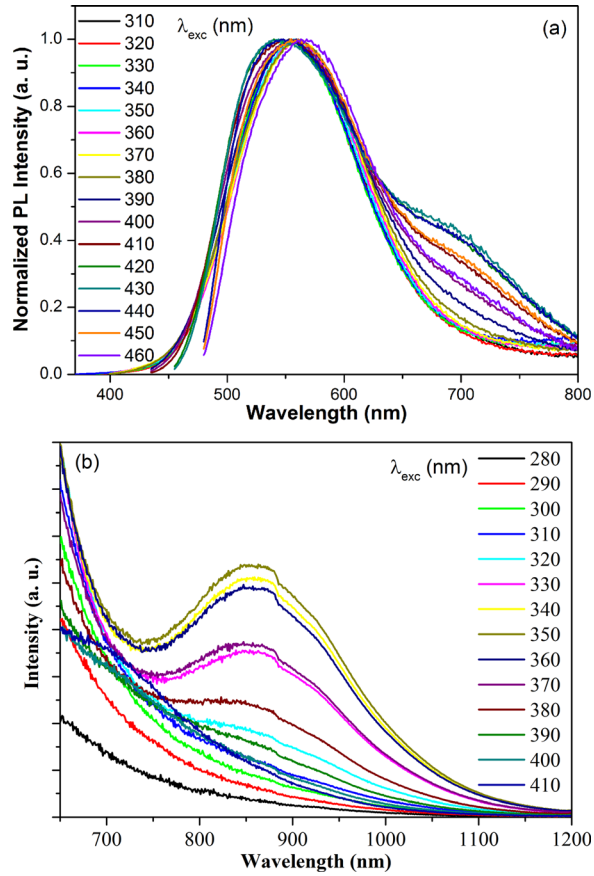

FIG. 5. Visible (a) and NIR (b) PL spectra for $S_{150\ mM\text{-}550\,^{\circ}C}$ under different excitation wavelengths.

may be attributed to the ~690 nm emission that becomes dominant instead of the ~560 nm emission upon the 457 nm excitation. Variation of the dominant emission peaks upon

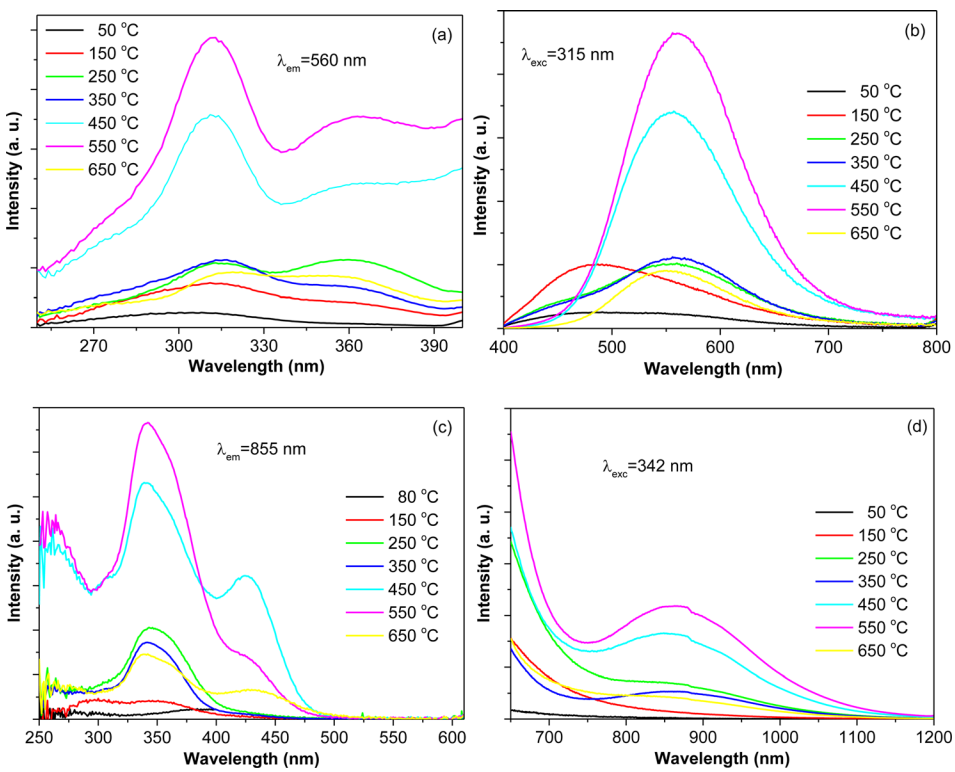

FIG. 4. PLE and PL spectra of the MLSCs activated zeolite A (the $S_{150\ mM\text{-}\times\times\times\,^{\circ}C}$ series) depending on the thermal activation temperatures.

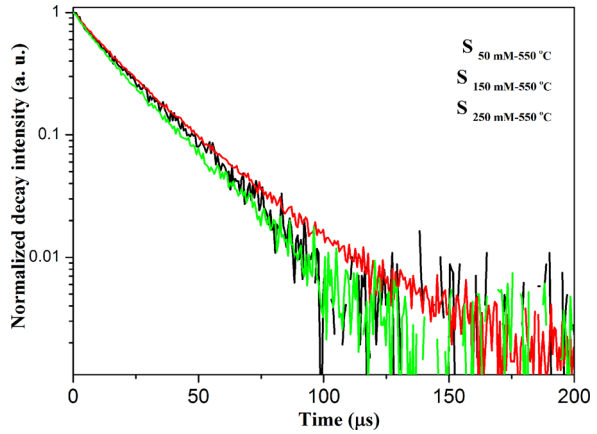

FIG. 6. Emission decay curves of the 855 nm emission from the MLSCs under the 355 nm excitation for $S_{50\ mM\text{-}550\,^{\circ}C}$, $S_{150\,mM\text{-}550\,^{\circ}C}$, and $S_{250\,mM\text{-}550\,^{\circ}C}$.

different excitation wavelengths has also been observed for the MLSCs confined in zeolite A.[22] In accordance with the visible PL, the peak position of the NIR emission is almost independent of the excitation wavelength.

The emission decay curves of the 855 nm emission for $S_{50\ mM\text{-}550\,^{\circ}C}$ and $S_{250\ mM\text{-}550\,^{\circ}C}$ both exhibit a single exponential decay, while the one for $S_{150\ mM\text{-}550\,^{\circ}C}$ exhibits a multi-exponential decay, as shown in Fig. 6. The mean emission lifetime of the ~855 nm emission for $S_{50\ mM\text{-}550\,^{\circ}C}$, $S_{150\,mM\text{-}550\,^{\circ}C}$, and $S_{250\ mM\text{-}550\,^{\circ}C}$ was 15 μs, 21 μs and 17 μs, respectively. The microsecond-scale emission life time indicates that the ~855 nm NIR emission is a spin-forbidden transition of one single kind of MLSC species. Interestingly, the ~855 nm NIR emission was not observed for the MLSCs confined in the zeolite Y matrix under the same preparation conditions, which may be attributed to the weak interaction between the silver ions/atoms. In zeolite Y, the Ag_2^+, Ag_3^+, and Ag_3^{2+}, etc., are also called "pseudo-clusters" due to the long Ag^0 (SI)-Ag^+ (SI′) bond lengths (3.1 Å vs. 2.89 Å for bulk silver).[30] The bond length for the linear Ag_3^{2+} trimers in the sodalite cage of zeolite A calculated from X-ray diffraction was 2.8–3.0 Å,[30] which provides a stronger interaction between the silver ions/atoms than the situation in zeolite Y.

CONCLUSIONS

Upon the 342 nm excitation, strong and broad band NIR luminescence peaked at ~855 nm has been observed from the MLSCs confined in the zeolite A matrix. This ~855 nm emission depends on the thermal activation temperature and the silver loading concentration. Judged by the steady/dynamic emission characteristics, the origin of this NIR emission is proposed to be a spin-forbidden transition of one single kind of luminescent MLSC species. This strong and broad NIR emission may have potential application as the down-converter layer to increase the conversion efficiency of crystalline solar cells.

[1]T. Vosch, Y. Antoku, J. C. Hsiang, C. I. Richards, J. I. Gonzalez, and R. M. Dickson, Proc. Natl. Acad. Sci. USA **104**, 12616 (2007).
[2]M. Eichelbaum and K. Rademann, Adv. Funct. Mater. **19**, 2045 (2009).
[3]A. Royon, K. Bourhis, M. Bellec, G. Papon, B. Bousquet, Y. Deshayes, T. Cardinal, and L. Canioni, Adv. Mater. **22**, 5282 (2010).
[4]G. De Cremer, B. F. Sels, J.-I. Hotta, M. B. J. Roeffaers, E. Bartholomeeusen, E. Coutiño-Gonzalez, V. Valtchev, D. E. De Vos, T. Vosch, and J. Hofkens, Adv. Mater. **22**, 957 (2010).
[5]M. C. Kanan, S. M. Kanan, and H. H. Patterson, Res. Chem. Intermed. States **29**(7–9), 691 (2003).
[6]W. S. Szulbinski, Inorg. Chim. Acta **269**, 253 (1998).
[7]Y. Miyamoto, T. Ohno, Y. Takei, H. Nanto, T. Kurobori, T. Yanagida, A. Yoshikawa, Y. Nagashima, and T. Yamamoto, Radiat. Meas. **55**, 72 (2013).
[8]Y. Miyamoto, T. Yamamoto, K. Kinoshita, S. Koyama, Y. Takei, H. Nanto, Y. Shimotsuma, M. Sakakura, K. Miura, and K. Hirao, Radiat. Meas. **45**, 546 (2010).
[9]S. Fedrigo, W. Harbich, and J. Buttet, J. Chem. Phys. **99**, 5712 (1993).
[10]A. Hoareau, P. Melinon, and B. Cabaud, J. Phys. D: Appl. Phys. **18**, 1731 (1985).
[11]C. I. Richards, S. Choi, J.-C. Hsiang, Y. Antoku, T. Vosch, A. Bongiorno, Y.-L. Tzeng, and R. M. Dickson, J. Am. Chem. Soc. **130**, 5038 (2008).
[12]H. X. Xu and K. S. Suslick, ACS Nano **4**, 3209 (2010).
[13]C. Guo and J. Irudayaraj, Anal. Chem. **83**, 2883 (2011).
[14]V. K. Tikhomirov, V. D. Rodríguez, A. Kuznetsov, D. Kirilenko, G. Van Tendeloo, and V. V. Moshchalkov, Opt. Express **18**, 22032 (2010).
[15]A. S. Kuznetsov, J. J. Velázquez, V. K. Tikhomirov, J. Mendez-Ramos, and V. V. Moshchalkov, Appl. Phys. Lett. **101**, 251106 (2012).
[16]H. Lin, D. Chen, Y. Yu, R. Zhang, and Y. Wang, Appl. Phys. Lett. **103**, 091902 (2013).
[17]T. Sun and K. Seff, Chem. Rev. **94**, 857 (1994).
[18]G. D. Cremer, Y. Antoku, M. B. J. Roeffaers, M. Sliwa, J. V. Noyen, S. Smout, J. Hofkens, D. E. D. Vos, B. F. Sels, and T. Vosch, Angew. Chem. Int. Ed. **47**, 2813 (2008).
[19]G. A. Ozin and F. Hugues, J. Phys. Chem. **87**, 94 (1983).
[20]G. D. Cremer, E. Coutiño-Gonzalez, M. B. J. Roeffaers, B. Moens, J. Ollevier, M. V. der Auweraer, R. Schoonheydt, P. A. Jacobs, F. C. De Schryver, J. Hofkens, D. E. De Vos, B. F. Sels, and T. Vosch, J. Am. Chem. Soc. **131**, 3049 (2009).
[21]L. R. Gellens, W. J. Mortler, R. A. Schoonheydt, and J. B. Uytterhoeve, J. Phys. Chem. **85**, 2783 (1981).
[22]E. Coutino-Gonzalez, M. B. J. Roeffaers, B. Dieu, G. D. Cremer, S. Leyre, P. Hanselaer, W. Fyen, B. Sels, and J. Hofkens, J. Phys. Chem. C **117**, 6998 (2013).
[23]Y. Chen, X. Zheng, X. Wang, C. Wang, Y. Ding, and X. Jiang, ACS Macro Lett. **3**, 74 (2014).
[24]X. Tu, W. Chen, and X. Guo, Nanotechnology **22**, 095701 (2011).
[25]J. T. Petty, C. Fan, S. P. Story, B. Sengupta, A. St. J. Iyer, Z. Prudowsky, and R. M. Dickson, J. Phys. Chem. Lett. **1**, 2524 (2010).
[26]J. T. Petty, C. Fan, S. P. Story, B. Sengupta, M. Sartin, J.-C. Hsiang, J. W. Perry, and R. M. Dickson, J. Phys. Chem. B **115**, 7996 (2011).
[27]A. Mathew, P. R. Sajanlal, and T. Pradeep, J. Mater. Chem. **21**, 11205 (2011).
[28]M. D. Baker, G. A. Ozin, and J. Godber, J. Phys. Chem. **89**, 305 (1985).
[29]A. Fielicke, I. Rabin, and G. Meijer, J. Phys. Chem. A **110**, 8060 (2006).
[30]L. R. Gellens, W. J. Mortler, and J. B. Uytterhoeve, Zeolites **1**, 11 (1981).
[31]H.-T. Sun, Y. Matsushita, Y. Sakka, N. Shirahata, M. Tanaka, Y. Katsuya, H. Gao, and K. Kobayashi, J. Am. Chem. Soc. **134**, 2918–2921 (2012).
[32]H.-T. Sun, Y. Sakka, N. Shirahata, Y. Matsushita, K. Deguchi, and T. Shimizu, J. Phys. Chem. C **117**, 6399–6408 (2013).